



COPY RIGHT



ELSEVIER
SSRN

2023 IJIEMR. Personal use of this material is permitted. Permission from IJIEMR must be obtained for all other uses, in any current or future media, including reprinting/republishing this material for advertising or promotional purposes, creating new collective works, for resale or redistribution to servers or lists, or reuse of any copyrighted component of this work in other works. No Reprint should be done to this paper, all copy right is authenticated to Paper Authors

IJIEMR Transactions, online available on 11th Sept 2023. Link

[:http://www.ijiemr.org/downloads.php?vol=Volume-12&issue=Issue 09](http://www.ijiemr.org/downloads.php?vol=Volume-12&issue=Issue 09)

10.48047/IJIEMR/V12/ISSUE 09/31

Title **CLOUD:GLOBAL NAVIGATION SATELLITE SYSTEM (GNSS) FOR GROUND MONITORING SYSTEM BASED ON IOT**

Volume 12, ISSUE 09, Pages: 256-262

Paper Authors **Dr.Sateesh Nagavarapu,Dr.Manam Vamsi Krishna, Babitha Kumari,Chandrakala Singh**



USE THIS BARCODE TO ACCESS YOUR ONLINE PAPER

To Secure Your Paper As Per **UGC Guidelines** We Are Providing A Electronic Bar Code



CLOUD:GLOBAL NAVIGATION SATELLITE SYSTEM (GNSS) FOR GROUND MONITORING SYSTEM BASED ON IOT

¹Dr.Sateesh Nagavarapu,² Dr.Manam Vamsi Krishna,³Babitha Kumari,⁴Chandrakala Singh

¹ Professor, ² Associate Professor, ^{3,4} Undergraduate student

^{1,2,3,4} Computer Science & Engineering

^{1,2,3,4} Malla Reddy Institute of Technology, Maisammaguda, Hyderabad-500100

¹sateeshnagavarapu@gmail.com,²manavamsikrishna@gmail.com,³kumaribabitha23@gmail.com,

⁴chandrakalasingh0707@gmail.com

Abstract:

Today's rapidly evolving invention, the Internet of Things, enables the integration of cutting-edge devices into systems. An intriguing opportunity to obtain ongoing information on the unusual and fleeting movement of ionosphere attributes with excessive wants is provided by using the Internet of things technology to collect data from a variety of Internet-connected GNSS beneficiaries. Making a thick sensor arrangement is made possible by using inexpensive single-recurrence GNSS receivers that rely on Arduino technology. It is possible to use this technology to continuously gather data on the ionosphere's overall total electron content. The assessment of the ionosphere TEC and the certain information of the ionosphere deferral to radio signal of Global positioning system satellite TV for PC are done simply within the Global navigation for system satellite benefit. The cloud server, where maps of the TEC to the ionosphere are created, receives the results via a remote correspondence medium over the Web. The proposed design that is now being suggested allows for direct data storage on the cloud. This design enables us to offer remote monitoring.

KEYWORDS: IOT-(Internet of Things), TEC-(Total Electron Content), GNSS (Global Navigation Satellite System), GPS- (Graphical Positioning System).

I. INTRODUCTION

The development of remote sensing has radically increased the amount of information obtained about processes taking place in the ionosphere and opened up new research areas for scientists. Absolute electrical substance is one of this ionosphere's characteristics. The change in Total Electronic Content indicates distinct processes taking place in the ionosphere, which is mirrored in the subsequent surface events. The use of the ground-based enrollment of radio signals by the global satellite network as part of an observation strategy, as well as the subsequent guarantee of the TEC of the ionosphere, depend on the

management of code and stage estimations of radio sign postponement.

The Arduino technology makes it possible to create unique, low-effort devices for the single-recurrence implementation technique for observing the entire electronic content of the ionosphere. This is a stage of openly programmable hardware that relies on the use of historical circuit sheets with a microcontroller. To produce a ground-based recipient, a GNSS module is associated with the card that approaches the internet via a remote Wi-Fi setup. The GNSS collector properly performs the confirmation of ionosphere deferral to radio sign and the computation of ionosphere TEC. Recently, the "Web of Things" innovation has been

productively producing. The Internet of Things is a reliable network of devices that uses hardware, software, and sensors. One can transmit all digital content information via a distant communication channel and process it independently without assistance from a human thanks to internet of things technology.

Revisions to the Global Navigation for System satellite positions are not always necessary for some packages, such as airborne assessment. For pc, estimates are gathered and handled for post-fundamental handling. Post-overseeing does not necessitate the predictable sending of differential modification messages, unlike RTK GNSS masterminding. The building plan is greatly enhanced by this. Base station data from at least one Global Navigation Satellite System beneficiary may be used during post-preparing. One of the major airborne applications is traversing vast areas with highly precise guardians of multi-base preparation.

Ground station data can frequently be unrestrictedly acquired, negating the necessity to build up your base station, dependent upon the undertaking's proximity to an eternity working GNSS coordinate. Without a base station, the data was downloaded using PPP, another feasible method, along with careful clock and hemisphere information. Programs for post-planning offer a wide range of adaptabilities. Applications can combine stationary or mobile base stations, various assistances that divert into an individual, and client or outcast programming modules. Applications that have been made ready for use may be suggested to run on PCs and open with simple graphical user interfaces.

II. BACKGROUND WORKS

In [1], the author explains how the use of IoT technology to compile data from several GNSS collectors connected to the Internet enables one of kind opportunities to get operational data about the dispersion of TEC with high spatial goals. The results are sent to a cloud administration via an Internet-based remote communication Channel. In [2] and [3], the creator used commercial FCSs, such as Pixhawk, which is important for using UAVs in everyday situations. The GNSS positioning options provided by commercial GNSS chips mounted on FCSs are suitable for UAVs flying two to three feet away from the ground. But, in urban areas with a large density of towering structures, it is not precisely enough to work safely in an aero plane.

Coordinating the GNSS system with the INS is one direct arrangement. Including the GNSS/INS based on the conventional Kalman channel plot has already enhanced locating. In light of this, the flexible Kalman channel was suggested to adjust the estimation procedure in an adaptive manner.

A few high-scope ionosphere model creations from the Polar Geophysical organization are discussed in [4]. The first is two-dimensional and depends on a strategy of transport conditions for five molecular species. The second, which is also three-dimensional, shows heated affects on the convective polar ionosphere. The two models were used to decode electron thickness images obtained using tomographic techniques during the 1993 Russian-American Tomographic Experiment, a 1995 Scandinavia, and a tomographic try in Russia in 1990.

The highlights of the F-district trough can be seen in the images of electron thickness that were previously introduced. On November 17, 1995, model counts of an

event observed during low daylight geomagnetic activity have been done. A circular shaped trough is visible in the sub aerial F-district on the tomographic image. The recreation demonstrates how the additional variables can result in such an example: (1) A latitudinal portion of the outer electric field with a top incentive is meridional. At trough scopes, up to 60 mV/m; (2) a steady zonal portion of the outer electric field with delicate electrons at the poleward end of the trough, with a typical molecular vitality of 0.3 keV.

Problem statement:

The IGS Network is used to download Figure 1. The maps are made up of numerous green dots, and each green dot represents a base station spread over the globe. All satellites send data to the base stations, where it is stored on the hard disc drives (HDD) that are housed in the base station servers.



Figure 1: Map showing the base Stations

There is a potential that an HDD failure or server crash will result in the loss of all incoming data. We therefore suggest a cloud-based architecture that will be practical and secure to prevent this kind of circumstance.

III. MATERIALS AND METHOD

Figure 2 depicts the base station's planned architecture when the satellite broadcasts the information that Node MCU will receive through the gateway. The gateway and the cloud are connected by the Node MCU. The data is processed and stored in the proper cloud to which it is connected after being received from the source. A data backup is also created on the server. The end user has remote access to the data kept in the cloud and can analyze the information received.

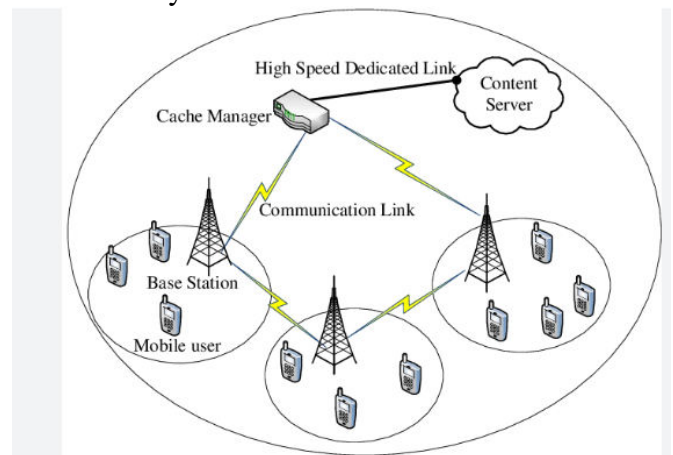


Fig.2 Proposal for the base station Architecture

Proposal for the base station Architecture:

The Node MCU, a GPS module, a power module, and the NEO M8 module for data storage make up the majority of this system. In Figure 2, the architecture is displayed. Once it is in control, the GPS module sets aside some effort to detect local nuances. Node MCU starts the web server and believes that a client will connect to it. Node MCU communicates location nuances to a consumer when they are connected to the web server. The location specifics are displayed in an easy-to-use HTML site page.

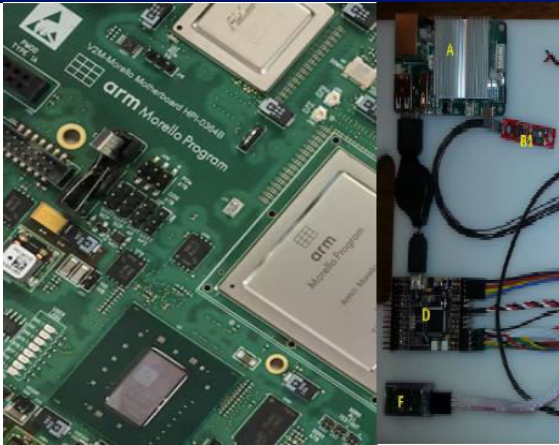


Fig.3 Hardware implementation of Proposed Architecture Prototype

1. Connect the circuit in the manner indicated by the schematic.
2. Move the code in response to changing Wi-Fi requirements.
3. It will highlight local nuances.
4. The sequential GPS module Neo 8M provides local nuances through sequential correspondence.

Pin	Description
Vcc	2.7-5 V power supply
Gnd	Ground
TXD	Transmit Data
RXD	Receive Data

Neo 8M GPS Module is TTL perfect and its details is given underneath

Capture Time	Cool Start:27s,Hot Start:1s
Communication Protocol	NMEA
Serial Communication	9600bps,8 data bits,1 stop bit, no parity and no flow control
Operating Current	45 mA

Location Data: This module can transmit data at a 9600 baud rate in a variety of

formats. If we use a UART terminal with a 9600 baud rate, we will be able to see statistics that were provided by GPS.

A global positioning system module uses an NMEA design to send real-time position updates. A few sentences make up the NMEA design, with four of them being particularly important. It may be possible to determine more details about the information organization.

GPGGA: Global Positioning system fix data

GPGSA: GPS satellites in view

GPRMC: Recommended minimum specific

GPS Transit data

NodeMCU	GPS module
3V3	VCC
GND	GND
D1(GPIO5)	RX
D2(GPIO4)	TX

Interfacing NEO 8M with NodeMCU

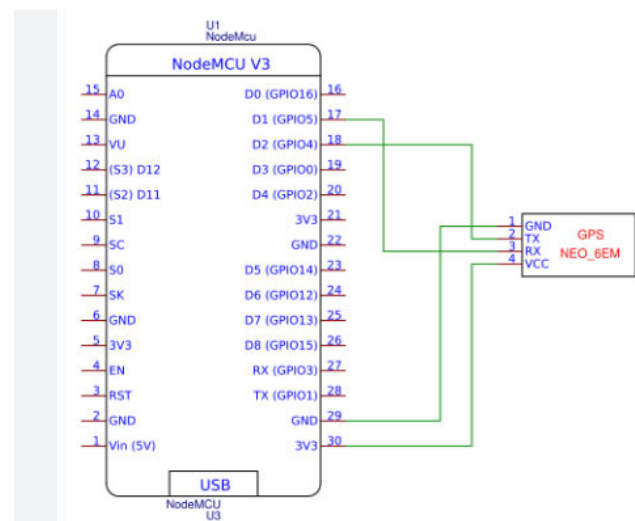


Fig.4. Circuit Diagram of interfacing GPS with Node MCU

The preparation of code and stage pseudo range estimations on a comparable carrier recurrence is necessary for a single

recurrence route beneficiary to guarantee the TEC of the ionosphere.

Finding the contrast between two progressive estimations is the key to the technique.

$$\Delta P_k - \Delta L_k = 80.8f - 2[m_i(\beta_k) - m_i(\beta_k - 1)]TEC$$

$$m_i(\beta_k) = \left[1 - \left[R \frac{\cos \beta_k}{R + Z_{max}} \right] 2 \right] - 0.5$$

$$TECK = TECK - 1 + K_k(\Delta P_k - \Delta L_k - HkTECK)$$

$$K_k = \frac{pkHk}{\sigma 2y}$$

$$Hk = 80.8f - 2[m_i(\beta_k) - m_i(\beta_k - 1)]$$

$$pk = \frac{[pk - 1 + \sigma 2x]}{[1 + (pk - 1 + \sigma 2x)H2k\sigma - 2y]}$$

IV. RESULTS AND DISCUSSION

We used Neo 8m interfaces with NodeMCU to implement the suggested prototype model at various locations and at various times, and then we exported the values to Thingspeak Cloud. The results are displayed below.

```

$GPSD,0000.00,0.00,00.00,00.00,00.00,00.00,M*30
$SDDBT,0.0,M,0.0,F,0.0,M,0.0,A,0.0
$SDZDA,21,02,10,14,30.00,00.00,M*31
$SDMTW,2.0,12.00,41.300,13.0,07.36,42.000,06.00,00.00,M*41
$SDMTD,2.0,12.00,41.300,13.0,07.36,42.000,06.00,00.00,M*42
$SDMTS,2.0,12.00,41.300,13.0,07.36,42.000,06.00,00.00,M*43
$SDMTL,2.0,12.00,41.300,13.0,07.36,42.000,06.00,00.00,M*44
$SDMTV,2.0,12.00,41.300,13.0,07.36,42.000,06.00,00.00,M*45
$SDMTA,2.0,12.00,41.300,13.0,07.36,42.000,06.00,00.00,M*46
$SDMTB,2.0,12.00,41.300,13.0,07.36,42.000,06.00,00.00,M*47
$SDMTX,2.0,12.00,41.300,13.0,07.36,42.000,06.00,00.00,M*48
$SDMTY,2.0,12.00,41.300,13.0,07.36,42.000,06.00,00.00,M*49
$SDMTZ,2.0,12.00,41.300,13.0,07.36,42.000,06.00,00.00,M*50
$SDMT1,2.0,12.00,41.300,13.0,07.36,42.000,06.00,00.00,M*51
$SDMT2,2.0,12.00,41.300,13.0,07.36,42.000,06.00,00.00,M*52
$SDMT3,2.0,12.00,41.300,13.0,07.36,42.000,06.00,00.00,M*53
$SDMT4,2.0,12.00,41.300,13.0,07.36,42.000,06.00,00.00,M*54
$SDMT5,2.0,12.00,41.300,13.0,07.36,42.000,06.00,00.00,M*55
$SDMT6,2.0,12.00,41.300,13.0,07.36,42.000,06.00,00.00,M*56
$SDMT7,2.0,12.00,41.300,13.0,07.36,42.000,06.00,00.00,M*57
$SDMT8,2.0,12.00,41.300,13.0,07.36,42.000,06.00,00.00,M*58
$SDMT9,2.0,12.00,41.300,13.0,07.36,42.000,06.00,00.00,M*59
$SDMT0,2.0,12.00,41.300,13.0,07.36,42.000,06.00,00.00,M*60
$SDMTA,2.0,12.00,41.300,13.0,07.36,42.000,06.00,00.00,M*61
$SDMTB,2.0,12.00,41.300,13.0,07.36,42.000,06.00,00.00,M*62
$SDMTX,2.0,12.00,41.300,13.0,07.36,42.000,06.00,00.00,M*63
$SDMTY,2.0,12.00,41.300,13.0,07.36,42.000,06.00,00.00,M*64
$SDMTZ,2.0,12.00,41.300,13.0,07.36,42.000,06.00,00.00,M*65
$SDMT1,2.0,12.00,41.300,13.0,07.36,42.000,06.00,00.00,M*66
$SDMT2,2.0,12.00,41.300,13.0,07.36,42.000,06.00,00.00,M*67
$SDMT3,2.0,12.00,41.300,13.0,07.36,42.000,06.00,00.00,M*68
$SDMT4,2.0,12.00,41.300,13.0,07.36,42.000,06.00,00.00,M*69
$SDMT5,2.0,12.00,41.300,13.0,07.36,42.000,06.00,00.00,M*70
$SDMT6,2.0,12.00,41.300,13.0,07.36,42.000,06.00,00.00,M*71
$SDMT7,2.0,12.00,41.300,13.0,07.36,42.000,06.00,00.00,M*72
$SDMT8,2.0,12.00,41.300,13.0,07.36,42.000,06.00,00.00,M*73
$SDMT9,2.0,12.00,41.300,13.0,07.36,42.000,06.00,00.00,M*74
$SDMT0,2.0,12.00,41.300,13.0,07.36,42.000,06.00,00.00,M*75
$SDMTA,2.0,12.00,41.300,13.0,07.36,42.000,06.00,00.00,M*76
$SDMTB,2.0,12.00,41.300,13.0,07.36,42.000,06.00,00.00,M*77
$SDMTX,2.0,12.00,41.300,13.0,07.36,42.000,06.00,00.00,M*78
$SDMTY,2.0,12.00,41.300,13.0,07.36,42.000,06.00,00.00,M*79
$SDMTZ,2.0,12.00,41.300,13.0,07.36,42.000,06.00,00.00,M*80
$SDMT1,2.0,12.00,41.300,13.0,07.36,42.000,06.00,00.00,M*81
$SDMT2,2.0,12.00,41.300,13.0,07.36,42.000,06.00,00.00,M*82
$SDMT3,2.0,12.00,41.300,13.0,07.36,42.000,06.00,00.00,M*83
$SDMT4,2.0,12.00,41.300,13.0,07.36,42.000,06.00,00.00,M*84
$SDMT5,2.0,12.00,41.300,13.0,07.36,42.000,06.00,00.00,M*85
$SDMT6,2.0,12.00,41.300,13.0,07.36,42.000,06.00,00.00,M*86
$SDMT7,2.0,12.00,41.300,13.0,07.36,42.000,06.00,00.00,M*87
$SDMT8,2.0,12.00,41.300,13.0,07.36,42.000,06.00,00.00,M*88
$SDMT9,2.0,12.00,41.300,13.0,07.36,42.000,06.00,00.00,M*89
$SDMT0,2.0,12.00,41.300,13.0,07.36,42.000,06.00,00.00,M*90
$SDMTA,2.0,12.00,41.300,13.0,07.36,42.000,06.00,00.00,M*91
$SDMTB,2.0,12.00,41.300,13.0,07.36,42.000,06.00,00.00,M*92
$SDMTX,2.0,12.00,41.300,13.0,07.36,42.000,06.00,00.00,M*93
$SDMTY,2.0,12.00,41.300,13.0,07.36,42.000,06.00,00.00,M*94
$SDMTZ,2.0,12.00,41.300,13.0,07.36,42.000,06.00,00.00,M*95
$SDMT1,2.0,12.00,41.300,13.0,07.36,42.000,06.00,00.00,M*96
$SDMT2,2.0,12.00,41.300,13.0,07.36,42.000,06.00,00.00,M*97
$SDMT3,2.0,12.00,41.300,13.0,07.36,42.000,06.00,00.00,M*98
$SDMT4,2.0,12.00,41.300,13.0,07.36,42.000,06.00,00.00,M*99
$SDMT5,2.0,12.00,41.300,13.0,07.36,42.000,06.00,00.00,M*00

```

Figure 5: Raw values received through NEO 8m interface



Figure 6: Data collected for 10 minutes early in the morning

The raw data obtained from the satellite and kept in the Thingspeak cloud are displayed in the graph above. Within a 30-second window, data is continuously changing. The time range shown on this graph is 6:45 AM to 6:55 AM.



Figure 7: Data collected for one Month. The time range in this graph, displayed in figure 7, is from 02/02/2020 to 02/03/2020. No data were gathered.



Figure 8: Graph data collected for 27 days duration

Figure 8 displays a graph. The time range is from 21 January 2020 to 27 January 2020. These days, data is not collected between



Figure 9: Graph shows the data collected for 30 minutes

The data in the graph above was gathered from 20:30 to 21:00. The graph fluctuates up and down because data changes continuously every 30 seconds.



Figure 10: Graph shows data collected in Different locations

Figure 10's top graph illustrates how data is gathered at various places using a NodeMCU-connected NEO M8 GPS module.

V. CONCLUSION

The base station sends data to the cloud when it receives data from the satellite, according to the paradigm we may suggest in this study. We collected the data from various GNSS receivers and uploaded it to the cloud. By using this design, users can simply monitor the data, and the data can be used effectively. Also, manpower will be minimized, and it will be simple to backup any lost data.

VI. REFERENCES

- [1].Olga Lazareva and Vladimir Chukin —Ground-Based GNSS Monitoring of Ionosphere as Implementation of Internet of Things Technology| Presented at the 2nd International Electronic Conference on Atmospheric Sciences, 16–31 July 2017.
- [2].GuohaoZhangLi-TaHsu —Intelligent GNSS/INS integrated navigation system for a commercial UAV flight control system Author links open overlay panell
- [3].Diomidis Spinellis. Position-annotated photographs: A geotemporal web. IEEE Pervasive Computing, 2(2):72–79, April-June 2003
- [4].Kunitsyn, V.E.; Tereshchenko, E.D.; Andreeva, E.S. Satellite radio probing and radio tomography of the ionosphere Radiotomogr. Ionos. 2007, 336, doi:10.3367/UFNr.0180.201005k.0548
- [5].K. Iwasaki, K. Yamazawa, and N. Yokoya. An indexing system for photos based on shooting position and orientation with geographic database. In IEEE



International Conference on Multimedia and Expo, ICME 2005, pages 390–393, 2005.

[6]. Ionosphere Correction Algorithm for Galileo Single Frequency Users. European GNSS (Galileo) Open Service—European Commission. 2016.

[7]. Krypiak-Gregorczyk, A., Wielgosz, P. and Borkowski, A. (2017a). Ionosphere Model for European Region Based on Multi-GNSS Data and TPS Interpolation. *Remote Sens.*, 9(12), 1221. DOI: 10.3390/rs9121221

[8]. Afifi, A.; El-Rabbany, A. Single Frequency Precise Point Positioning Using GPS and Galileo Observables, FIG Congress, Enhancing the Relevance Kuala Lumpur, Malaysia. 2014.

[9]. Sanz Subirana, J et al. (2013). —GNSS Data Processing – Vol. I: Fundamentals and Algorithms. European Space Agency (ESA). Noordwijk, The Netherlands.

[10]. Rahemi, N et al. (2014). —Accurate Solution of Navigation Equations in GPS Receivers for Very High Velocities Using Pseudorange Measurements. *Adv in Aerospace Eng*, 2014, Article ID 435891, 8 pages.

[11]. Kinal, G.V. and Singh, J.P. (1990) An International Geostationary Overlay for GPS and GLONASS. *Navigation*, Vol. 37, No. 1. US Institute of Navigation, Cambridge, Mass.

[12]. Evers, H., Kahmann, H. and Kasties, G. (1993) Differential GPS in a Land Vehicle Environment. *Proceedings DSNS 93*, Netherlands Institute of Navigation, Amsterdam.

[13]. Kasties, H., Han, Y. and Lechner, W (1993) Realization of Real-time DGPS Receiver-Mix. *Proceedings of the ION National Technical Meeting 6/93*, US Institute of Navigation, Cambridge, Mass.